

Preparation of a [70]fullerene-ZnO nanocomposite in an electric furnace and photocatalytic degradation of organic dyes

Sung Kyu Hong, Jeong Ho Lee, Bum Hwi Cho and Weon Bae Ko*

Department of Chemistry, Sahmyook University, Seoul 139-742, South Korea

A [70]fullerene-ZnO nanocomposite was synthesized by a solid-state reaction between a synthesized ZnO and [70]fullerene in an electric furnace at 700 °C. The morphology and optical properties of the ZnO nanoparticles, [70]fullerene, heat treated [70]fullerene and the [70]fullerene-ZnO nanocomposite were characterized by UV-vis spectroscopy, X-ray diffraction (XRD), scanning electron microscopy (SEM) and transmission electron microscopy (TEM). The tendency of photocatalytic activity of several nanomaterials such as [70]fullerene, heat treated [70]fullerene and the [70]fullerene-ZnO nanocomposite to degrade organic dyes which were methylene blue (MB), methyl orange (MO), rhodamine B (RhB) was investigated by UV-vis spectroscopy.

Key words: [70]Fullerene-ZnO nanocomposite, Electric furnace, Photocatalytic activity, Organic dyes, UV-vis spectroscopy.

Introduction

Fullerenes have attracted considerable attention owing to their unique electronic properties in material sciences associated with fullerene chemistry [1]. Fullerenes contain an extensively conjugated three-dimensional π system. For example, C₆₀ has a closed-shell configuration consisting of 30 bonding molecular orbitals with 60 π -electrons, which is suitable for an efficient electron transfer reduction due to minimal changes in the structure and solvation associated with the electron transfer [2]. It has been proposed that an intramolecular photoprocess (electron or energy transfer) can occur between the peripheral fullerene subunit and the central core. Some studies have reported that fullerenes can efficiently cause rapid photoinduced charge separation and relatively slow charge recombination [2, 3].

ZnO nanoparticles are a wide-band-gap semiconductor (3.37 eV) with a large exciton binding energy of 60 meV [4], and have attracted a great deal of attention in various fields, such as solar cells [5], gas sensors [6], light emitting diodes [7], optoelectronic devices [8] and photocatalysts for environmental remediation owing to their non-toxicity and eco-friendliness [9]. ZnO nanoparticles are well established and there has been abundant interest since their wide-band-gap mainly absorbs the UV-light in application areas of photocatalysts [10]. ZnO nanoparticles are a promising photocatalyst for the degradation of organic dyes in an aqueous solution. The photocatalysis process of ZnO nanoparticles under UV-light irradiation has been used successfully to degrade pollutant dyes for the past

few years [11-17]. However, the solar UV-light reaching the earth's surface that can excite TiO₂ is relatively small (\approx 4%), and artificial ultra-violet light sources are somewhat expensive. The biggest advantage of ZnO is that it absorbs a larger fraction of the solar spectrum than TiO₂ [18]. The combination of excellent photocatalytic properties of ZnO and efficient electron transfer of [70]fullerene appears to be ideal for enhancing the photon efficiency.

This paper reports the successful synthesis of ZnO nanoparticles and [70]fullerene-ZnO nanocomposites. In addition, the photocatalytic activity of each nanomaterial, [70]fullerene, heat treated [70]fullerene and the [70]fullerene-ZnO nanocomposite, in organic dyes, such as MB, MO and RhB under UV-light at 254 nm was studied by UV-vis spectroscopy.

Experimental

Chemicals

[70]Fullerene was purchased from Nanobest Corp. Zn(NO₃)₂·6H₂O, NaOH, tetrahydrofuran and ethanol were obtained from Samchun Chemicals. The organic dyes (MB, MO and RhB) were supplied by Sigma-Aldrich.

Instruments

The morphology and crystallite size of the synthesized ZnO nanoparticles, [70]fullerene, heat treated [70]fullerene and the [70]fullerene-ZnO nanocomposite were examined by TEM (JEOL Ltd, JEM-2010) at an acceleration voltage of 200 kV. The structures of the nanomaterials were determined by XRD (Rigaku, Rigaku DMAX PSCC MDG 2000). All sample surfaces were observed by SEM (Hitachi S4700) at an accelerating voltage between 0.5 and 15 kV. UV-vis spectra were obtained using a UV-vis spectrometer (Shimadzu UV-1601PC). All samples were

*Corresponding author:
Tel : +82-2-3399-1700
Fax: +82-2-979-5318
E-mail: kowb@syu.ac.kr

treated under continuous ultrasonic irradiation using an ultrasonic generator UGI1200 (Hanil Ultrasonic Co., Ltd.) with a frequency of 20 kHz and a normal power of 750 W. The ultrasonic generator was a horn type system with a horn tip diameter of 13 mm. An electric furnace (Ajeon Heating Industry Co., Ltd.) was used to heat the samples. An ultra-violet lamp (8 W, 254 nm, 77202 Marne La Valee-cedex 1 France) was used as the ultraviolet light irradiation source.

Synthesis

Preparation of ZnO nanoparticles

10 M NaOH and 1.0 M $Zn(NO_3)_2 \cdot 6H_2O$ were dissolved in 6 ml of distilled water. 15 ml of ethanol was then added to each sample. After mingling the two solutions in a beaker, this solution was placed under ultrasonic irradiation for 45 minutes at room temperature. The solution which accomplished the reaction under ultrasonic irradiation at room temperature was removed and the white precipitate at the bottom of the beaker was purified by distilled water and ethanol (99%), and dried at room temperature [19].

Preparation of nanomaterials for evaluating photocatalytic effect

The heat treated [70]fullerene was placed separately into a vessel and heated in an electric furnace to 700 °C under Ar for 2 hours. After the heat treatment, samples were cooled to room temperature under Ar for 4 hours. The ZnO nanoparticles and [70]fullerene were placed into a vial containing 10 ml of tetrahydrofuran to produce

the [70]fullerene-ZnO nanocomposite. The vial was then stirred vigorously at room temperature for 1 hour. The mixed solution was poured into a vessel and dried for 2 hours to evaporate the organic solution. The vessel containing the mixture was placed into an electric furnace and heated to 700 °C under Ar for 2 hours. The sample was then cooled to room temperature under Ar for 4 hours.

Degradation of organic dye with nanomaterials

The [70]fullerene, heat treated [70]fullerene and the [70]fullerene-ZnO nanocomposite were used as catalysts to degrade the MB, MO and RhB. 10 mg of each nanomaterial was placed into a vial containing 10 ml of 0.01 M organic dye solution. The [70]fullerene and heat treated [70]fullerene were irradiated with ultra-violet light at 254 nm for per an hour but the [70]fullerene-ZnO nanocomposite was illuminated with an ultra-violet lamp at 254 nm for one minute. The organic dye degraded by each nanomaterial under ultra-violet light was characterized by UV-vis spectroscopy.

Results and Discussion

ZnO nanoparticles were prepared via an ultrasonication process of a zinc nitrate and sodium hydroxide solution at room temperature for 45 minutes. The ZnO nanoparticles were characterized by UV-vis spectroscopy, XRD, TEM and SEM, and their results are shown in Fig. 1. The synthesized ZnO nanoparticles were dispersed in distilled water to determine the position of the peak value of ZnO

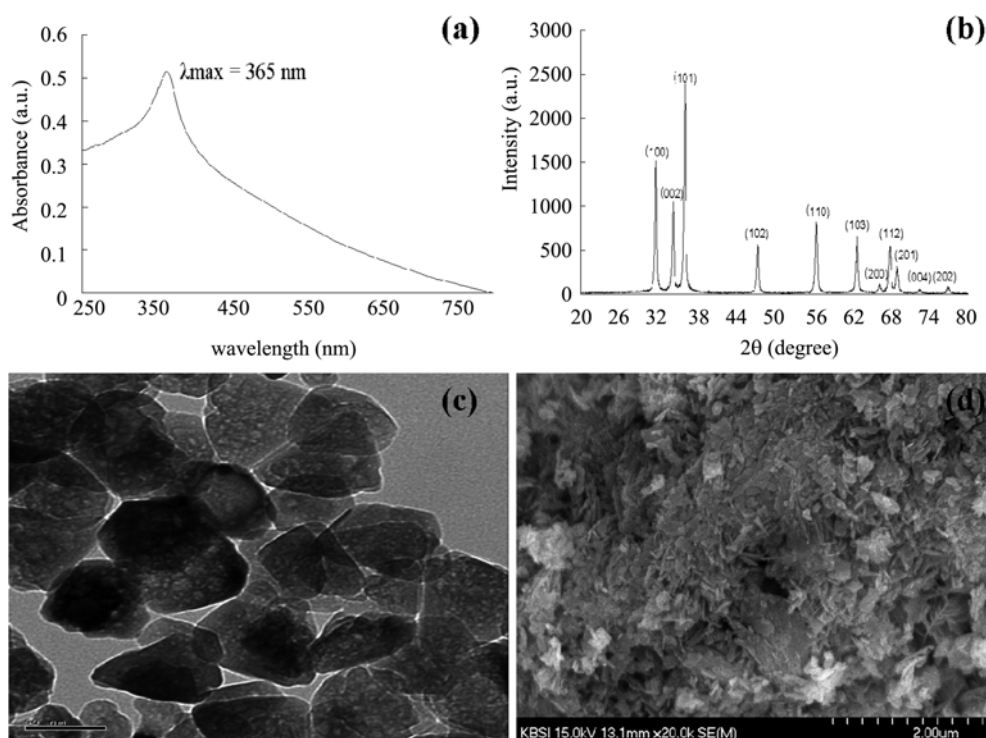


Fig. 1. UV-vis spectrum (a), XRD pattern (b), TEM image (c), and SEM image (d) of synthesized ZnO nanoparticles formed under ultrasonic irradiation.

nanoparticles. Fig. 1(a) shows that the peak of ZnO nanoparticles occurs at $\lambda_{\max} = 365$ nm. Fig. 1(b) shows the XRD peaks of the ZnO nanoparticles synthesized under ultrasonic irradiation for 45 minutes. These studies were performed using a powder of ZnO nanoparticles. The characteristic peaks for ZnO nanoparticles at ($2\theta = 31.71, 34.37, 36.19, 47.47, 56.49, 62.33, 66.33, 67.81, 68.99, 72.47, 76.85$), marked by indices [(100), (002), (101), (102), (110), (103), (200), (112), (201), (004), (002)] confirm that the resulting ZnO nanoparticles were crystalline. The ZnO nanoparticles showed no XRD peaks from impurity phases. Fig. 1(c) shows a TEM image of the ZnO nanoparticles. The synthesized ZnO nanoparticles showed a number of shapes which were trigonal, hexagonal and spherical, and most of the synthesized ZnO nanoparticles had an average size of 50 nm. In addition, the ZnO nanoparticles were porous, which would make it easier to adsorb chemical products on their surfaces. Fig. 1(d) shows a SEM image of the synthesized ZnO nanoparticles. An inhomogeneous structure of ZnO nanoparticles is apparent and most ZnO nanoparticles had a needle-like shape.

The [70]fullerene was purchased from the Sigma-Aldrich cooperation and characterized by UV-vis spectroscopy, XRD, TEM and SEM. Fig. 2(a) and (b) present the UV-vis spectra (a) of [70]fullerene in tetrahydrofuran and an XRD pattern (b), respectively. The [70]fullerene exhibited a peak intensity approximately at 9.60, 10.20, 10.86, 14.02, 16.66, 18.12, 19.58, 19.92, 20.44 as a 2θ value. Each XRD peak of the [70]fullerene was indexed [(110), (002), (101), (102), (110), (103), (112), (201), (004)] [20] confirming its crystallinity. Fig. 2(c) shows a TEM image of

[70]fullerene. Fig. 2(c) shows the shapes of [70]fullerene particles, such as trigonal, spherical, hexagonal and tetragonal. Most of the [70]fullerene had a spherical structure. The SEM image of [70]fullerene showed a flat surface (Fig. 2(d)).

The heat treated [70]fullerene was prepared in an electric furnace under Ar at 700 °C for two hours. This material was characterized by UV-vis spectroscopy, XRD, TEM and SEM (Fig. 3). Fig. 3(a) shows that the heat treated [70]fullerene by UV-vis spectra, was similar to the [70]fullerene. From the result of the UV-vis spectra, the optical properties of the [70]fullerene were not changed by the high temperature. In addition, XRD (Fig. 3(b)) of heat treated [70]fullerene showed few changes except for the sharp and narrow diffraction peaks. The product showed good crystallinity and purity. XRD of the heat treated [70]fullerene showed that the heat treatment removed the impurity materials. Fig. 3(c) shows a TEM image of the [70]fullerene heat treated using an electric furnace under Ar at 700 °C for two hours. The amorphous shape of [70]fullerene was attributed to the breaking of [70]fullerene crystals by the heat treatment using an electric furnace. The amorphous shape of the [70]fullerene meant that a high temperature caused the fragmentation of the crystalline material. Therefore, most of the heat treated [70]fullerene had a spherical shape. Fig. 3(d) shows a SEM image of the [70]fullerene. As expected, most of the [70]fullerene surfaces had a porous, inhomogeneous shape. The treatment at high temperature led to an increase in the surface area of the material through an increase in porosity.

Fig. 4 shows the UV-vis spectra, XRD, TEM and SEM

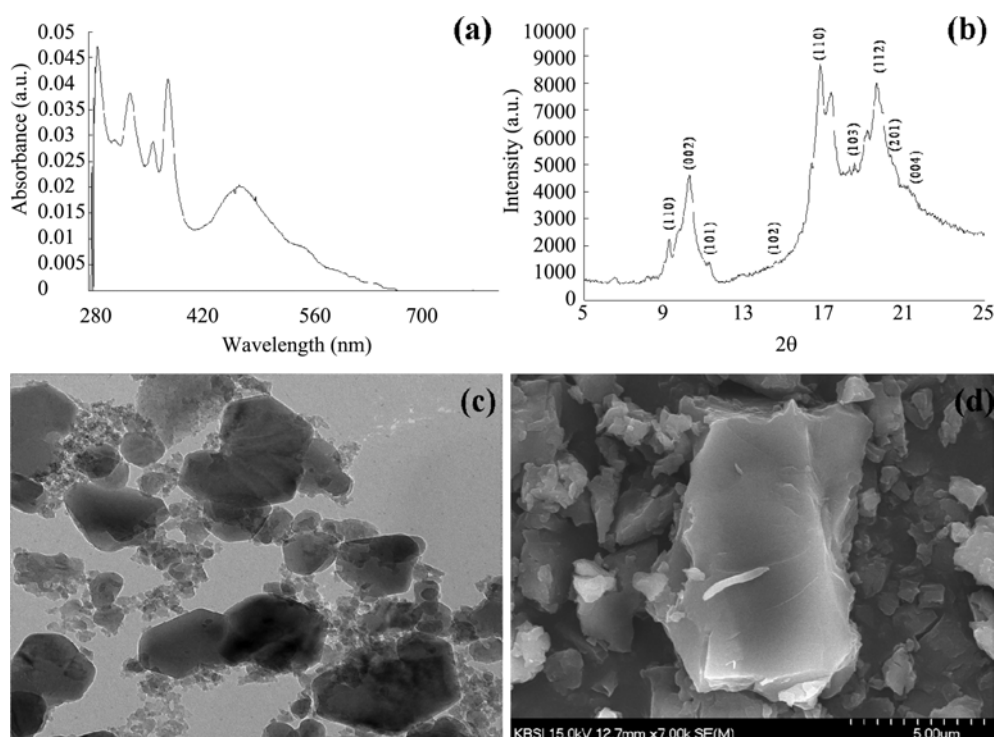


Fig. 2. UV-vis spectrum (a), XRD pattern (b), TEM image (c), and SEM image (d) of [70]fullerene.

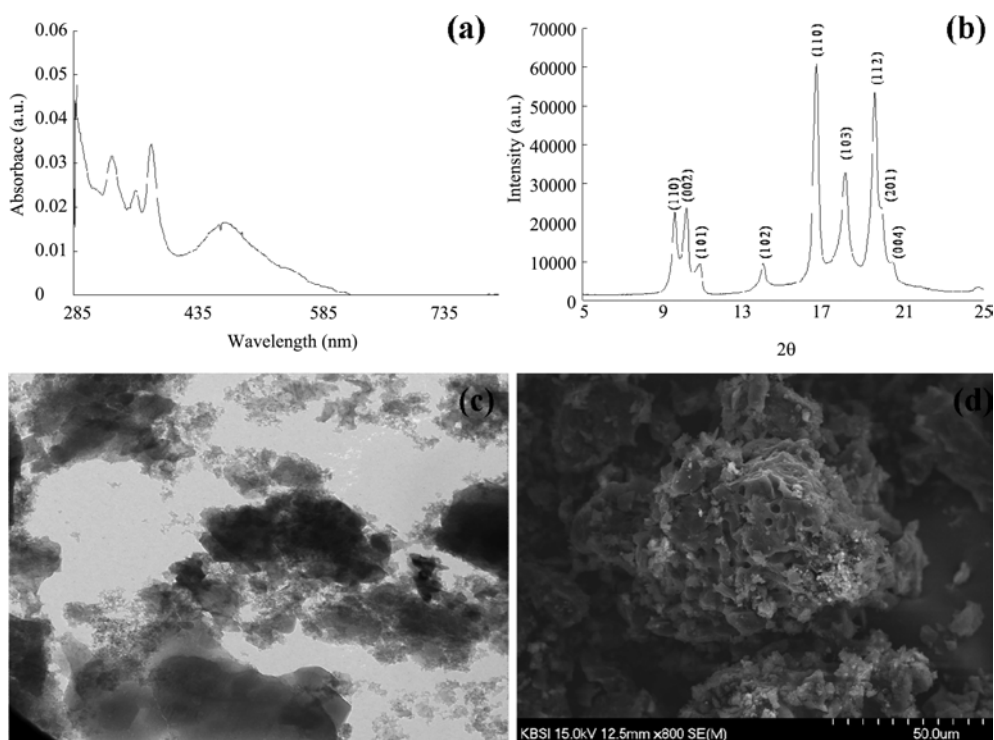


Fig. 3. UV-vis spectrum (a), XRD pattern (b), TEM image (c), and SEM image (d) of [70]fullerene heat treated by an electric furnace at 700 °C for two hours.

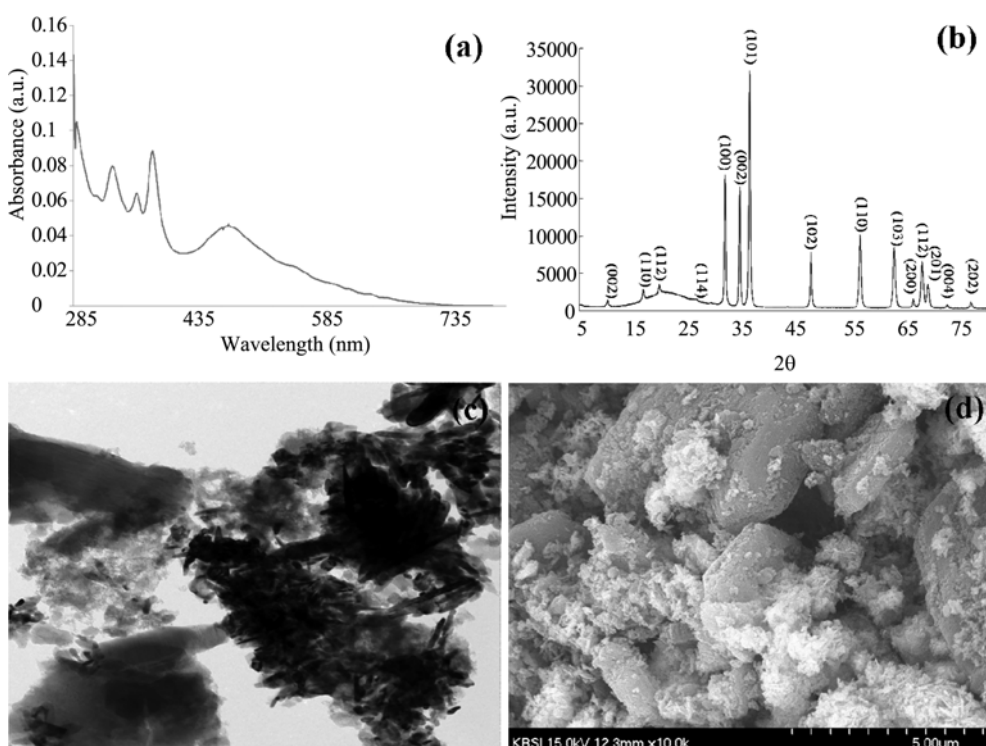


Fig. 4. UV-vis spectrum (a), XRD pattern (b), TEM image (c), and SEM image (d) of the [70]fullerene-ZnO nanocomposite heat treated by an electric furnace at 700 °C for two hours.

characterization of the [70]fullerene-ZnO nanocomposite. The [70]fullerene-ZnO nanocomposite was prepared by heating in an electric furnace under Ar at 700 °C for two

hours. UV-vis spectra under ultra-violet light at 254 nm confirmed the photocatalytic effect. Fig. 4(a) presents the UV-vis spectrum of the [70]fullerene-ZnO nanocomposite

in tetrahydrofuran. The peaks of the [70]fullerene-ZnO nanocomposite were observed at 288 nm, 314 nm, 332 nm, 360 nm, 380 nm and 470 nm in the UV-vis spectra. These peaks were attributed to character of the [70]fullerene. Fig. 4(b) shows the XRD pattern of the [70]fullerene-ZnO nanocomposite. The X-ray diffraction peaks of the [70]fullerene-ZnO nanocomposite was seen 10.30, 16.80, 19.72, 26.64, 31.78, 34.44, 36.26, 47.56, 56.62, 62.88, 66.40, 67.98, 69.14, 72.66, 77.00 as 2θ values and marked by plane indices [(002), (110), (112), (114), (100), (002), (101), (102), (110), (103), (200), (112), (201), (004), (202)], respectively. The XRD peaks value of 10.30, 16.80, 19.72, 26.64 as a 2θ value were attributed to the [70]fullerene and the residual peaks were assigned to the ZnO nanoparticles. Fig. 4(c) shows a TEM image of the [70]fullerene-ZnO nanocomposite. The ZnO nanoparticles were agglomerated and their surfaces were made porous by the treatment at high temperature. The fragment of [70]fullerene made by the electric furnace under Ar at 700 °C for two hours was surrounded by ZnO nanoparticles. ZnO nanoparticles in the [70]fullerene-ZnO nanocomposite showed a rod

shape, with a porous structure on the surfaces of the ZnO nanoparticles. Fig. 4(d) shows a SEM image of the [70]fullerene-ZnO nanocomposite. The ZnO nanoparticles in the [70]fullerene-ZnO nanocomposite had a needle-like shape, and the [70]fullerene in the [70]fullerene-ZnO nanocomposite appeared as fragmented and broken crystals after the heat treatment in the electric furnace under Ar at 700 °C for two hours.

Fig. 5, 6 and 7 show the degradation of the organic dyes, such as MB, MO and RhB with [70]fullerene, heat treated [70]fullerene and the [70]fullerene-ZnO nanocomposite as a photocatalyst under ultra-violet irradiation at 254 nm. The degradation of organic dyes, such as MB, MO and RhB, using [70]fullerene, heat treated [70]fullerene under UV irradiation were measured for one hour by UV-vis spectroscopy. The heat treated [70]fullerene showed a faster degradation tendency for the organic dyes than the other. However, the [70]fullerene-ZnO nanocomposite was irradiated with ultra-violet light for one minute. This photocatalyst showed much higher efficiency for degrading the organic dyes under ultra-violet light at 254 nm. The

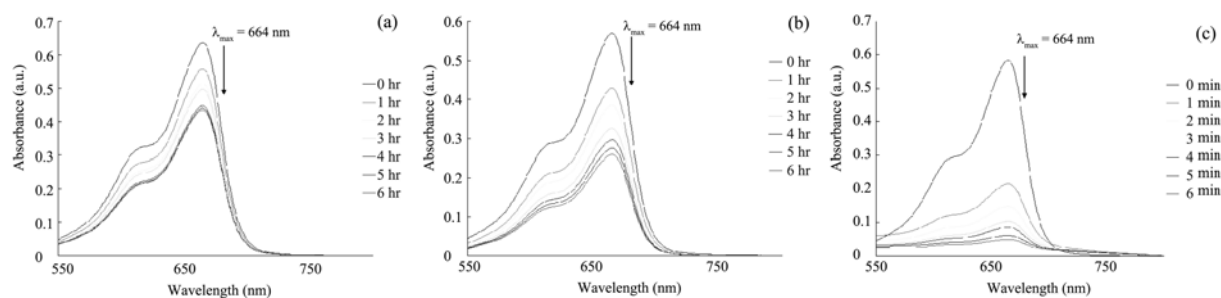


Fig. 5. UV-vis spectra of methylene blue with various photocatalysts under a UV-lamp at 254 nm; [70]fullerene (a), heat treated [70]fullerene (b), [70]fullerene-ZnO nanocomposite (c).

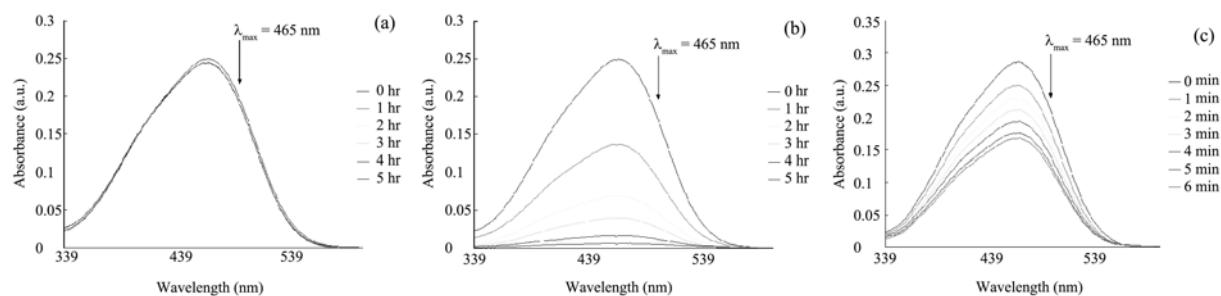


Fig. 6. UV-vis spectra of methyl orange with various photocatalysts under a UV-lamp at 254 nm; [70]fullerene (a), heat treated [70]fullerene (b), [70]fullerene-ZnO nanocomposite (c).

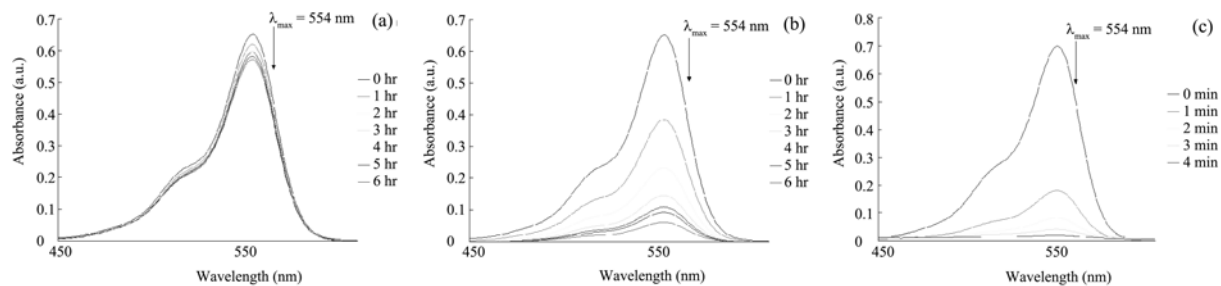


Fig. 7. UV-vis spectra of rhodamine B with various photocatalysts under a UV-lamp at 254 nm; [70]fullerene (a), heat treated [70]fullerene (b), [70]fullerene-ZnO nanocomposite (c).

reason for the efficiency of the [70]fullerene-ZnO nanocomposite was due to the increased surface area of the photocatalyst by the electric furnace and a change to rod shape and fragments. These results would make it easier to adsorb the organic dyes on the surface of the photocatalyst and degrade the organic dyes. In addition, the [70]fullerene-ZnO nanocomposite had a synergistic effect in degrading the organic dyes under ultra-violet light, for each nanomaterial which was [70]fullerene and ZnO nanoparticles [21] showed good efficiency as a photocatalyst in degrading the organic dyes under ultra-violet light. The [70]fullerene-ZnO nanocomposite was showed a good tendency to degrade MB, RhB under ultra-violet light.

Conclusions

Ultrasonication is a good method for synthesizing ZnO nanoparticles. Each photocatalyst was prepared by heat treatment in an electric furnace under Ar at 700 °C for two hours except for the [70]fullerene sample. TEM and SEM imaging of [70]fullerene and ZnO nanoparticles showed that the shape of each photocatalyst was changed by the high temperature heat treatment. The shape of [70]fullerene was altered from large particles to small fragmented particles and the shape of the ZnO nanoparticles changed from needle-like to rod-like. In addition, each photocatalyst had a porous structure caused by the heating process. The photocatalytic activity of [70]fullerene, heat treated [70]fullerene and the [70]fullerene-ZnO nanocomposite for the degradation of MB, MO, and RhB under UV light at 254 nm was examined by UV-vis spectroscopy. The [70]fullerene-ZnO nanocomposite was more effective in the photocatalytic degradation of the organic dyes as a photocatalyst than the other materials examined. Further studies will be made of how these nanomaterials can be used in practical waste water treatment.

References

1. R.C. Haddon, Science 261 (1993) 1545-1550.

2. T. Hasobe, S. Hattori, P.V. Kamat and S. Fukuzumi, Tetrahedron 62 (2006) 1937-1946.
3. S. Zhu, T. Xu, H. Fu, J. Zhao and Y. Zhu, Environ. Sci. Technol. 41 (2007) 6234-6239.
4. J.J. Wu and S.C. Liu, Adv. Mater. 14 (2002) 215-218.
5. A. Belaidi, Th. Dittrich, D. Kieven, J. Tomow, K. Schwarzburg, M. Kunst, N. Allsop, M.-Ch. Lux-Steiner and S. Gavrilov, Sol. Energy. Mater. Sol. Cells 93 (2009) 1033-1036.
6. J. Joo, D. Lee, M. Yoo and S. Jeon, Sens. Actuators B. 138 (2009) 485-490.
7. D.C. Kim, W.S. Han, B.H. Kong, H.K. Cho and C.H. Hong, Physica B. 401 (2007) 386-390.
8. M. Purica, E. Budianu and E. Rusu, Microelectron. Eng. 51 (2000) 425-431.
9. C. Hariharan, Appl. Catal. A: Gen. 304 (2006) 55-61.
10. D.D. Dionysiou, M.T. Suidan, E. Bekou, I. Baudin and M.J. L  n  , Appl. Catal. B 26 (2000) 153-171.
11. K.K. Ioannis and A.A. Triantafyllos, Appl. Catal. B: Environ. 49 (2004) 1-14.
12. A. Akyol, H.C. Yatmaz and M. Bayramoblu, Appl. Catal. B: Environ. 54 (2004) 19-24.
13. C.G. Silva and J.L. Faria, J. Photochem. Photobiol. A: Chem. 155 (2003) 133-143.
14. D. Yu, R. Cai and Z. Liu, Spectrochem. Acta A 60 (2004) 1617-1624.
15. A. Akyol and M. Bayramoglu, J. Hazard. Mater. B 124 (2005) 241-246.
16. M.J. Height, S.E. Pratsinis, O. Mekasuwandumrong and P. Praserthdam, Appl. Catal. B: Environ. 63 (2006) 305-312.
17. K. Mehrotra, G.S. Yablonsky and A.K. Ray, Ind. Eng. Chem. Res. 42 (2003) 2273-2281.
18. I. Poullos and I. Tsachpinis, J. Chem. Technol. Biotechnol. 74 (1999) 349-357.
19. R.S. Yadav, P. Mishra and A.C. Pandey, Ultrason. Sonochem. 15 (2008) 863-868.
20. C.S. Sundar, P. Ch. Sahu, V.S. Sastry, G.V.N. Rao, V. Sridharan, M. Premila, A. Bharathi, Y. Hariharan, T.S. Radhakrishnan, D.V.S. Muthu and A.K. Sood, Phys. Rev. B 53 (1996) 8180-8183.
21. S.K. Hong, G.Y. Yu, C.S. Lim and W.B. Ko, Elast. Compos. 45 (2010) 206-211.